AD-A054 971 RCA LABS PRINCETON N J F/G 20/3
REPRODUCIBLE ADHESION TEST FOR SOLDERED THICK-FILM CONDUCTORS.(U)
JUL 77 T T HITCH N00163-76-C-0287
UNCLASSIFIED PRRL-77-CR-38 NL

1 OF 1
AD A054971

END
DATE FILMED
7-78
DDC

UNCLASSIFIED

SECURITY CLASSIFICATION OF THIS PAGE (When Data Entered)

REPORT DOCUMENTATION PAGE	READ INSTRUCTIONS BEFORE COMPLETING FORM
1. REPORT NUMBER	2. GOVT ACCESSION NO. 3. RECIPIENT'S CATALOG NUMBER
4. TITLE (and Subtitle) REPRODUCIBLE ADHESION TEST FOR SOLDERED THICK-FILM CONDUCTORS.	5. TYPE OF REPORT & PERIOD COVERED Final Report 30 JUN 76-30 JUN 77
	6. PERFORMING ORG. REPORT NUMBER PRRL-77-CR-38
7. AUTHOR(s) Thomas T. Hitch	8. CONTRACT OR GRANT NUMBER(s) N00163-76-0287 new N00163-76-C-0287
9. PERFORMING ORGANIZATION NAME AND ADDRESS RCA Laboratories Princeton, New Jersey 08540	10. PROGRAM ELEMENT, PROJECT, TASK AREA & WORK UNIT NUMBERS
11. CONTROLLING OFFICE NAME AND ADDRESS Naval Avionics Facility Indianapolis, Indiana 46206	12. REPORT DATE 31 Jul 1977
	13. NUMBER OF PAGES 45 P.
14. MONITORING AGENCY NAME & ADDRESS (if different from Controlling Office)	15. SECURITY CLASS. (of this report) Unclassified
	15a. DECLASSIFICATION/DOWNGRADING SCHEDULE N/A

16. DISTRIBUTION STATEMENT (of this Report)

DISTRIBUTION STATEMENT A
Approved for public release;
Distribution Unlimited

17. DISTRIBUTION STATEMENT (of the abstract entered in Block 20, if different from Report)

18. SUPPLEMENTARY NOTES

19. KEY WORDS (Continue on reverse side if necessary and identify by block number)

Reproducible adhesion test
Thick-film conductors
Failure-mode analysis
Adhesion data conversion
Soldered-wire test

20. ABSTRACT (Continue on reverse side if necessary and identify by block number)

The need for an adhesion test method that is more reproducible from operator to operator and from laboratory to laboratory is well known in the thick-film industry. The development of such a method was begun at RCA under earlier Naval contracts, and has been completed and tested in detail in this study. Thorough descriptions of two recommended variations of the method, the apparatus required to

over

DD FORM 1 JAN 73 1473

UNCLASSIFIED

SECURITY CLASSIFICATION OF THIS PAGE (When Data Entered)

299000 kc

20.

perform them, and the evaluations made during this study are presented.

The soldered-wire peel test was adopted as the focal point of the study because of its widespread acceptance by the industry. A range of dimensions for the elements of test parts was studied, and the ideal ranges of dimensions were established. Test pad sizes of 0.1 in. x 0.1 in. and 0.08 in. x 0.08 in. and a 0.032-in. wire diameter lie within the ideal size ranges.

A major object of the study plan was to eliminate possibilities for the adhesion-test-specimen assembler to influence the results of the tests. Accordingly, the developed test method controls (1) the relative positions of the wire and pad by jigging them, (2) the amounts of solder and flux by preplacing measured quantities, and (3) the time/temperature history by the use of controlled-temperature hot air for the soldering. Other phases of specimen preparation and testing are similarly controlled.

Where the method was used for samples of identically prepared films, the standard deviation divided by the arithmetic mean of the group was found to approach 10 pct if the films were moderately to strongly adherent and if the failure mode was an adhesion failure, i.e., a clean film-from-substrate separation. Other failure modes and their interpretations are discussed.

A variation of the test method is presented that is based on the use of an indium-containing solder and was developed under the contract for use with gold films. The suggested standard method is suitable for Ag, Ag-Pd, Au-Pd, Au-Pt, Au-Pt-Pd, Cu, and Ni metallizations; 62Sn-36Pb-2Ag (wt pct) solder is used.

Information is supplied to aid the first-order comparison of adhesion data taken by the use of the developed test with data taken by the thermocompression-bonded peel test.

PREFACE

This final report describes work performed in the Integrated Circuit Technology Center of RCA Laboratories, under Contract No. N00163-76-C-0287. Mr. J. H. Scott, Jr., is the Laboratory Director and Dr. G. L. Schnable, the Project Supervisor and Group Head. Dr. Thomas T. Hitch is the Project Scientist and with Mr. E. J. Conlon comprises the principal research team. Mr. William Musgrave is the Government Project Monitor.

It is a pleasure to acknowledge the help of a number of individuals in RCA who have contributed to this study. Notable are John O'Droniec for design of the bend fixture; C. Morris for help with the electroforming design; and J. Avins, K. Bube, R. DeStephanis, K. Hang, and T. Shelton for useful discussions. Consultation with Dr. G. L. Schnable throughout the study and his review of the manuscript have been most valuable.

We acknowledge helpful discussions with the scientists and engineers studying adhesion test technology at Sandia Laboratories, the Naval Research Laboratories, and several ink manufacturing companies; with the Project Monitor, Mr. Bill Musgrave, and his supervisor, Mr. Stephen Hart; and with others at Naval Avionics Facility, Indianapolis.

TABLE OF CONTENTS

LIST OF ILLUSTRATIONS

LIST OF ILLUSTRATIONS (Continued)

LIST OF TABLES

SECTION I

INTRODUCTION

The need for adhesion testing is widely recognized. Such tests are necessary to make comparisons of both materials and the effects of processing on material properties. In the thick-film industry, a particular need has developed for a reproducible test that can be adopted by a large fraction of the industry. The adhesion testing of thick-film conductor materials was reviewed recently by this author [1] and is, consequently, not reviewed here. Several other authors have reviewed the topic [2,3] or have described individual tests that they found of value [4-7]. One group of the workers has been studying test configurations designed to yield values of adhesion strength in terms of G_{IC}, the fracture energy in pure tension. However, the test-specimen preparations for their tests are time-consuming, and interpretation of the data occasionally has proved to be difficult [8,9].

---

1. T. T. Hitch, "Adhesion Measurements on Thick Film Conductors," in K. L. Mittal, Ed., *Adhesion Measurements of Thin Films, Thick Films and Bulk Coatings*, to be published by ASTM, Philadelphia, PA.
2. L. Jacobson, "Testing for Adhesion of Hybrid Films," *Proc. IEEE and EIA Electronic Components Conf., 1971*, p. 474.
3. R. P. Anjard, "Thick Film Conductor Adhesion Testing," *Microelectron. Reliability* 10, 269 (1971).
4. S. S. Leven," Qualification Requirements for Thick-Film Networks," ECOM Final Report No. ECOM-73-0326-F, by Westinghouse D&E Systems Center, Baltimore, MD, Oct. 1975.
5. D. R. Johnson and R. E. Knutson, "Parallel Gap Welding to Thick-Film Metallization," *IEEE Trans. Parts, Hybrids, and Packaging* PHP-12, 187 (1976).
6. A. C. Buckthorpe, "Degradation of Thick Film Conductor Adhesion," *IERE Conf. Hybrid Microelectron., 1973*, p.57.
7. T. H. Lemon, "High Tensile Strength Thick-Film Silver-Palladium Metallizations *IERE Conf. Hybrid Microelectron., 1975*, p.23.
8. P. F. Becher et al., "Fracture Mechanics Approach to Thick Film Adhesion Testing," *Proc. Int. Microelectron. Symp. (ISHM), 1975*, p.279.
9. P. F. Becher and J. S. Murday, "Factors Affecting Thick Film Adhesion," *Proc. Int. Microelectron. Symp. (ISHM), 1976*, p.235.

SECTION II

DEVELOPMENT OF THE TEST METHOD

A. SELECTION OF THE APPROACH

The choice of test methods to be studied under the contract was made on the basis of many factors. These included the pertinence of test part and loading configurations to hybrid-circuit designs, simplicity of test design, ease of test-specimen fabrication and testing, and expected acceptability of the method by the thick-film hybrid community. The method selected was the soldered-wire peel test, for which two major variations have been advocated in the literature [3,10]. The du Pont-advocated configuration [10] is shown in Fig. 1. Anjard's method [3] is similar, except that he employed a test-pad size of 0.10 in. x 0.10 in. instead of 0.080 in. x 0.080 in.

Our experience with the use of the 0.10-in. x 0.10-in. pad variation in a study series for the Naval Air Systems Command [11-13] showed that it could deliver highly reproducible data, but that care was needed to avoid variation in the test specimens.

A primary objective in the development of a reproducible test is to reduce, as far as possible, any subjective influence that the operator might have on test-specimen assembly. Variation in the amount of solder, in the thermal shocking of test specimens, and in temperature excursions caused by soldering with an iron, as well as the generally poor thermal and geometric specimen-to-specimen consistency, were considered the principal factors for which improvement was required.

---

10. E. I. du Pont De Nemours & Co., Inc., "Method of Test for Wire Peel Adhesion of Soldered Thick Film Conductors to Ceramic Substrates," *The Thick Film Handbook*, Section A-74672, Wilmington, DE, March 1971.
11. T. T. Hitch and K. R. Bube, "Basic Adhesion Mechanisms in Thick and Thin Films," Final Report, NASC Contract No. N00019-C-74-0270, 31 Jan. 1975.
12. T. T. Hitch and K. R. Bube, "Basic Adhesion Mechanisms in Thick and Thin Films," Final Report, NASC Contract No. N00019-75-C-0145, 30 Jan. 1976.
13. K. R. Bube and T. T. Hitch, "Basic Adhesion Mechanisms in Thick and Thin Films," Final Report, NASC Contract No. N00019-76-C-0256, 31 Jan. 1977.

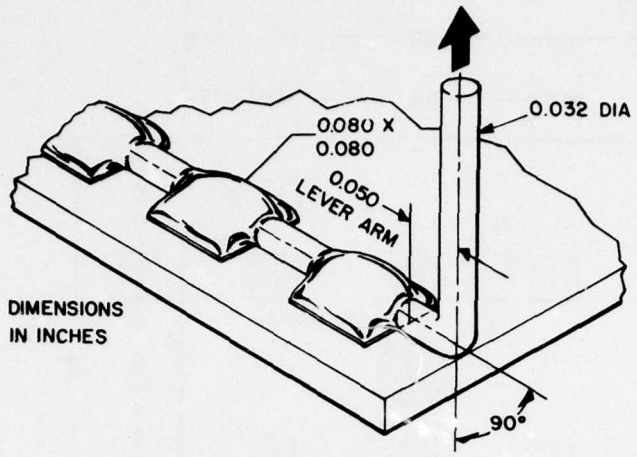

Figure 1. Soldered-wire peel adhesion test (after du Pont).

To solder specimens more uniformly, a source of heat was sought that would allow rapid, uniform heating of the entire substrate at once. A controlled-temperature air stream was chosen as the method of heat application.

Another problem in the general use of the soldered-wire peel test methods is that the pull wire extends beyond the pad being tested to others that will be tested subsequently. This problem is correlated with du Pont's private statement that they test only the first of the four pads in each row of their test pads. In a study at RCA [13], a lot of assembled test specimens was thermally aged for 500 h at 150°C. Upon removal of the specimens from the oven, the differential thermal-expansion coefficient between the substrate and the copper wire connecting the pads caused many test-pad failures before testing. To eliminate the stressing of test pads by testing of adjacent pads, to allow testing of thermally aged samples, and to maximize the number of good test pads on a substrate, it was decided that we would cut the wires between test pads on all subsequent specimens for this test.

B. DESCRIPTION OF TEST SPECIMENS AND THE APPARATUS FOR THEIR ASSEMBLY

A conductor test pattern, designed for this study, accommodated both the use of a hot-air heat source for soldering and the decision to not attempt successive tests along a row of test pads. The pattern is shown in Fig. 2. It contains four pads for adhesion testing plus arrow points to indicate the corner of the printer nest into which the substrate was registered for alignment. The four test pads are located symmetrically about the center of the substrate to ensure that each will experience the same time/temperature cycle.

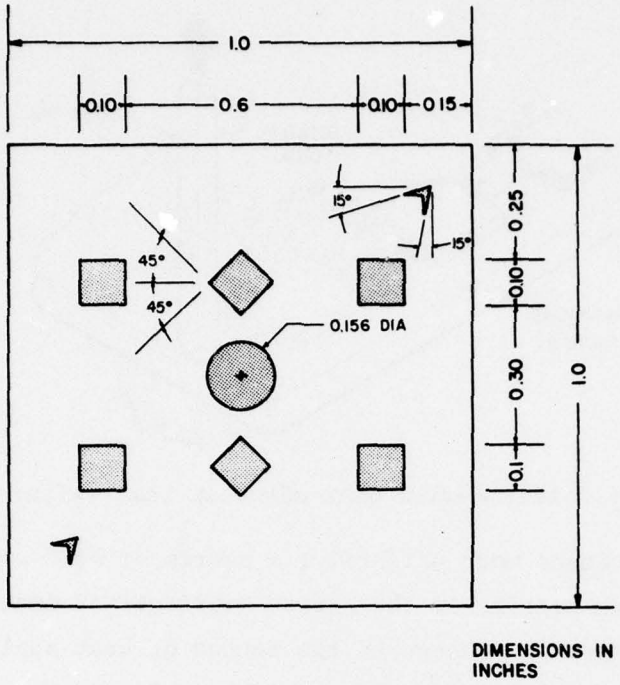

Figure 2. Conductor adhesion test pattern with four test pads.

The diagonally oriented and circular pads were used for wire-alignment checks and for attaching thermocouples to study the substrate thermal cycle.

The apparatus for specimen fabrication is shown in Fig. 3.

Pull wires of soft-annealed copper wire* were chosen because of the tendency for solder to wet the wire too far beyond the test pad when pretinned wires were employed.

The 62Sn-36Pb-2Ag solder** was chosen for use with most conductors because of its versatility. It can be used with high-silver-content conductors, as well as most other conductors that can be soldered with Sn-Pb solders.

The use of a hot-air blast to solder implies prepositioning of the specimen components for soldering. Furthermore, the specimen-to-specimen geometrical

*Specifications for the copper wire, a suitable vendor for it, and similar details for other commercially available parts are given in the Appendix.
**Solder compositions are given in percent by weight (wt pct).

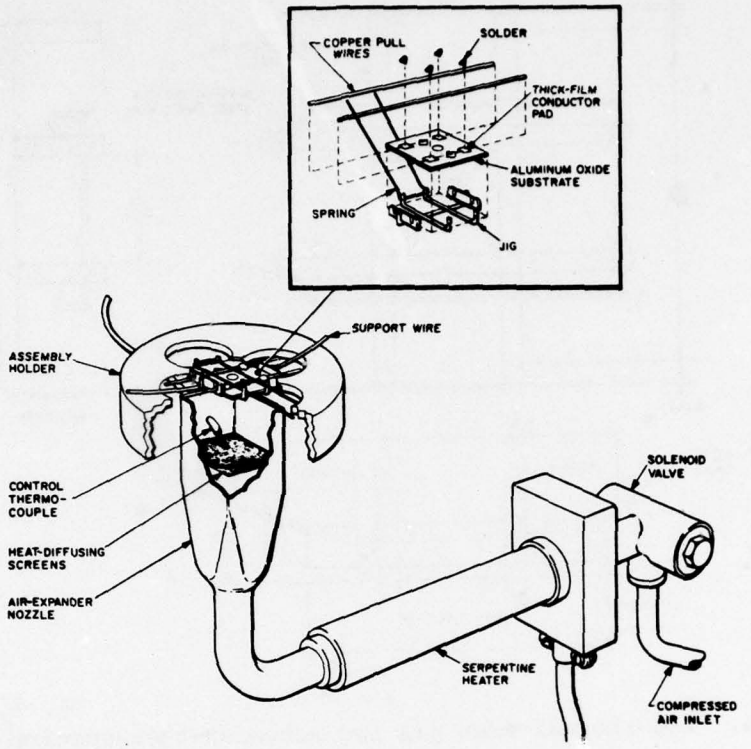

Figure 3. Adhesion-test-specimen assembly: apparatus and fixtures.

uniformity that can be obtained by "jigging" the parts for soldering is desirable. A low-thermal-mass jig to hold the copper wires over the conductor pads was developed. This is illustrated isometrically in Fig. 3 and in two-dimensional detail in Fig. 4. The grooves in the fixture and careful alignment of the pattern on the substrates are required to center the wires over the test pads. The force of the spring wire against the copper wire ensures that the copper wire will lie directly against the conductor metallization after the solder solidifies (i.e., a uniform spacing will be achieved). We had sought a method for the straightforward fabrication of test specimens with a small uniform spacing of the wire off the conductor pad surface [14] but finally chose direct contact for simplicity and speed of specimen production. In use, the jigged assembly of substrate and copper wires are placed in the

14. E. J. Conlon, R. DeStephanis, and T. T. Hitch, U.S. Pat. 3,972,463 (1976) (RCA Corp.).

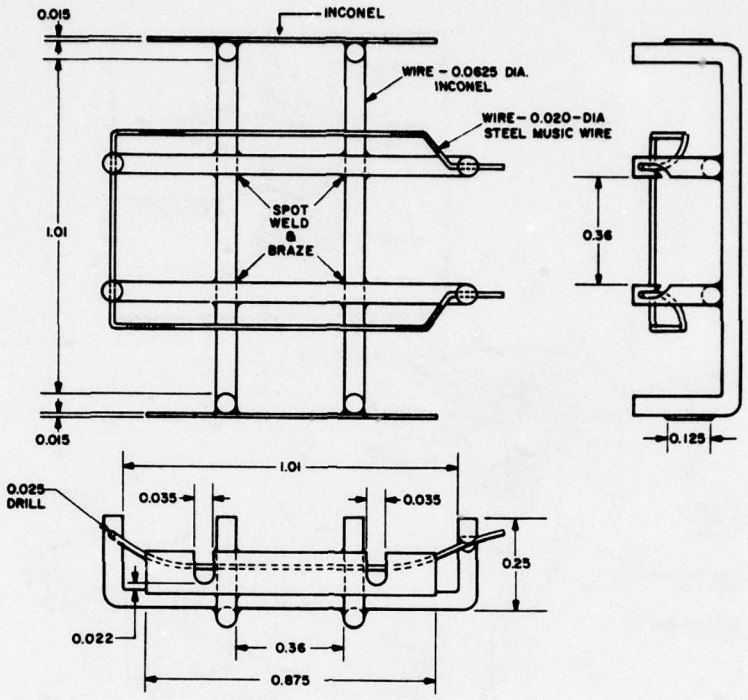

Figure 4. Low-thermal-mass jig for adhesion-test-specimen assembly.

assembly holder (for dimensional detail, see Fig. 5), and a spring support - an 0.040-in.-diameter tungsten wire - (shown in Fig. 3) is slipped under the jigged assembly to lift the substrate corners into the positioning notches of the assembly holder. The assembly holder is made of Pyrex* to minimize heat conduction from the substrate. It is positioned so that its upper face is 0.525 in. from the expander nozzle.

The solenoid valve controls the flow of house-compressed air through the Sylvania Serpentine II Heater.** The air stream expands through the nozzle and the velocity profile is leveled by the heat-diffusing screens. The electrodeposition form for the air-expansion nozzle that was developed under the contract is shown in Fig. 6.

*Registered Trademark of the Corning Glass Co., Corning, NY.
**GTE Sylvania, Inc., Exeter, NH.

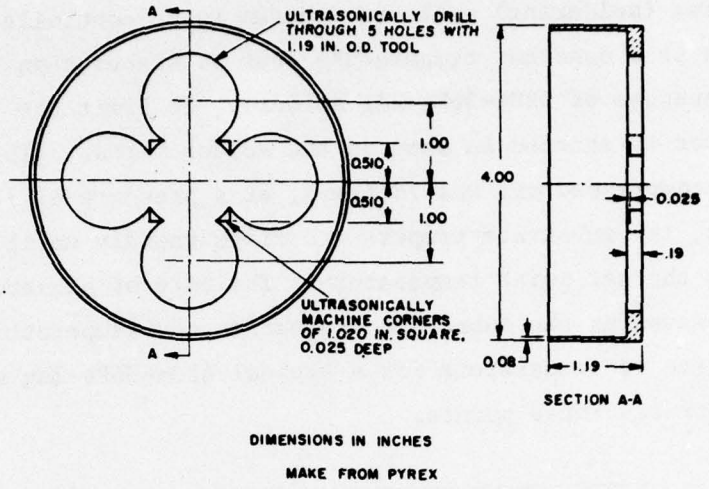

Figure 5. Adhesion-test-specimen assembly holder.

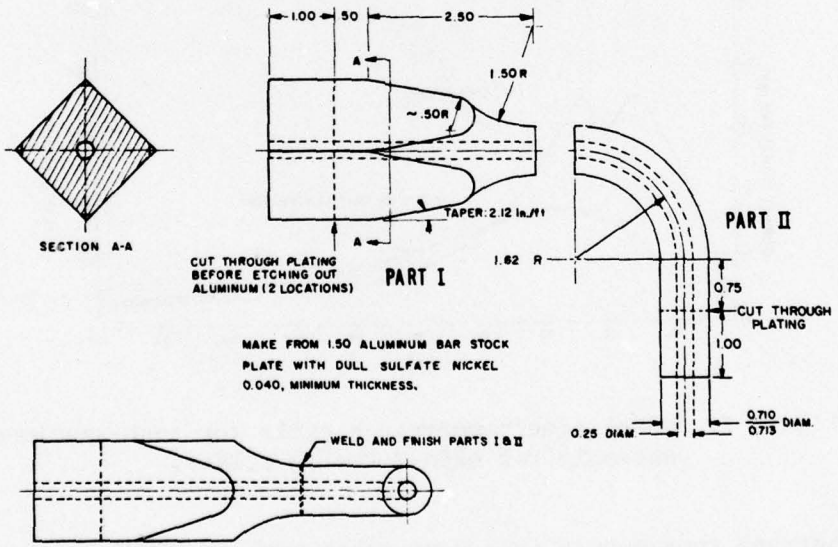

Figure 6. Air-expander electroforming mandrel. (Dimensions in inches.)

The major problem in direct control of specimen temperature was in achieving a high specimen production rate. After several unsuccessful attempts to sense temperature and control it directly from the test specimen substrate, the control thermocouple was located in the air-expansion nozzle.

C. DEVELOPMENT OF THE SOLDER CYCLE

The heating (soldering) cycle was chosen to be controlled by heating of the air stream to a constant temperature that is higher than 179°C (the liquidus temperature of 62Sn-36Pb-2Ag solder). To limit the time of further heating, a timer is started as soon as the solder melts. (The flow-rate of unheated, house-compressed air was 78 L/min, at a pressure of 75 lb/in.^{2}.) With this procedure, the substrate temperature rises rapidly until the air in the nozzle reaches the set point temperature. The rate of substrate temperature rise then decreases as the substrate approaches the temperature of the air. The graph of time vs temperature for a typical 62Sn-36Pb-2Ag soldering cycle (Fig. 7) illustrates these points.

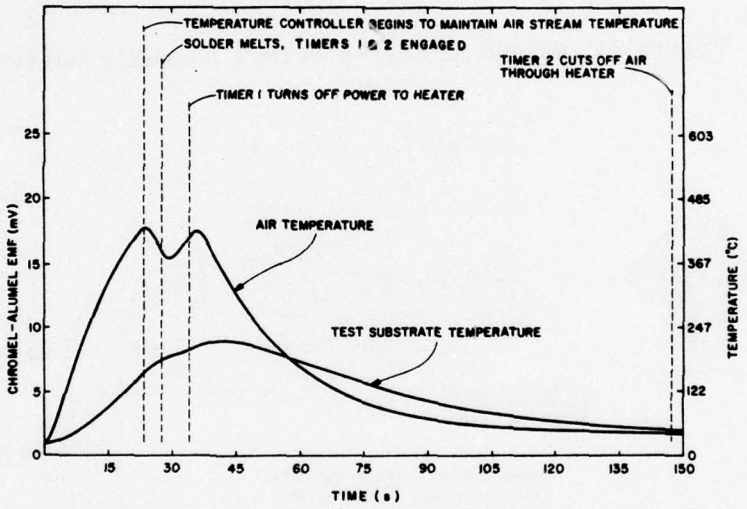

Figure 7. Model time/temperature cycle for test-specimen assembly for 62Sn-36Pb-2Ag solder.

The substrate temperature data were taken with an 0.005-in.-diameter-wire, chrome-alumel thermocouple soldered with Alpha* Alloy 112 (liquidus temperature of 238°C) to the round center metallization pad in the substrate test pattern (Fig. 2). It was noted that problems arose due to irregular wetting of the

*Alpha Metals, Inc., Jersey City, NJ.

conductor pads. For uniformity of the test method from conductor material to conductor material and to achieve the best uniformity within specimen lots, it was decided, reluctantly, to employ the manual operations of burnishing, dipping (tinning) in a temperature-controlled solder pot, and wiping to remove excess solder. Since burnishing is a common industry practice, the adhesion-test data should be consistent with standard hybrid-circuit practice. Particularly where difficult-to-solder Au-Pt-(Pd) and Ag-Pd conductors are used, burnishing must be employed to achieve uniform wetting without the use of inappropriately active fluxes.

D. ASSEMBLY OF THE TEST SPECIMEN

1. Recommended Standard Procedure

A procedure has been developed for solder assembly of adhesion-test parts. The 62Sn-36Pb-2Ag alloy is suitable for most thick-film materials that are normally considered solderable (i.e., Au-Pt, Au-Pd, Au-Pt-Pd, Ag, Ag-Pd, Ag-Pt, Cu, and Ni thick-film conductors). The same schedule should be used by persons who prefer to employ 63Sn-37Pb solder, since the melting/liquidus temperatures of these two solders are only a few degrees apart. However, since 63Sn-37Pb rapidly dissolves most Ag, Ag-Pt, and some Ag-Pd thick films, RCA recommends that 62Sn-36Pb-2Ag be employed as the standard solder in the adhesion testing of thick-film conductors, as described below:

(1) Screen, dry, and fire the conductor test patterns, as shown in Fig. 4, onto 1-in. x 1-in. x 0.025-in. substrates.

(2) Burnish the substrate surface* to ensure complete wetting by the solder.

(3) Dip the substrate in mildly activated rosin flux** (Kester† 1544).

(4) Immerse in a temperature-controlled solder pot at 210 $\pm$ 2°C for 5 s (62Sn-36Pb-2Ag solder).

---

*In our work we used a "3-in-1" burnishing eraser, manufactured by Fancourt Industries, Brooklyn, NY.

**A more active flux may be required for use with nickel metallizations.

†Kester Solder Co., Chicago, IL.

(5) While the solder is still molten, and with a minimum of delay, wipe all excess solder from the substrate.

(6) Remove the flux residue by soaking the substrate in trichloroethylene.

(7) Dip the cleaned substrates in nonactivated-rosin solder flux (Alpha 100), predry in air at room temperature, and bake dry at 125°C for 30 min.* Parts can now be stored indefinitely without loss of solderability.

(8) Place two annealed 0.032-in. diameter, oxygenfree, high-conductivity (OFHC) copper wires** and the substrate into a low-thermal-mass jig that positions the wires, each against two of the thick-film test pads and centered over them.

(9) Place the jigged assembly into a holder which positions it over the Sylvania Serpentine II heat source and air-expander nozzle.†

(10) Place a fixed volume (0.031-in. diameter x 0.25-in. long), vee-shaped piece of 62Sn-36Pb-2Ag solder wire over the copper wire on each test pad.

(11) Flux each pad with 7 μL of mildly activated rosin flux (Kester 1544).

(12) Heat the jigged assembly through the controlled temperature-time cycle described earlier.

(13) Remove the flux residue by soaking the substrate in trichloroethylene.

(14) Reject, before testing, any soldered-wire test pads that do not appear uniform. (For example, too much or too little solder, the pull wire lying off center on the test pad, or poor wetting of pad.)

(15) Bend up the wires to conform to the test geometry†† (0.050 in. from center of wire to edge of pad).

(16) Cut the copper wires from between adjacent pads.

(17) Wait at least 24 hours to allow stress relaxation in the solder.

(18) Test in a hard-beam test machine at 0.5 in./min crosshead speed.

---

*Step 7 may be eliminated if the test substrate is not to be stored in the tinned condition for a significant amount of time.

**Atlantic Brass and Copper Co., Linden, NJ.

†A design for an electroformed nozzle is shown in Fig. 6.

††A simple fixture to facilitate the bending is described under II.E.

2. Procedure Variation for Gold Conductors

Neither 62Sn-36Pb-2Ag nor 63Sn-37Pb solder is satisfactory for use on gold thick-film conductors. A modification of the Sn-Pb system by the ternary addition of indium produces a solder that does not leach gold significantly. Indalloy* Solder No. 9, with composition 70Sn-18Pb-12In, used with Indalloy No. 4 Electro (rosin) flux gives a reasonably priced eutectic system that is straighforward to use. It is stronger than most of the other indium alloy solders and, in particular, is more than 50% stronger than the popular 50Pb-50In. Indalloy No. 9 had proved useful for adhesion tests on gold in earlier work at RCA [15].

The soldering schedule given in Table 1 for 62Sn-36Pb-2Ag solder imposes on the substrate the time-temperature cycle described in Fig. 7. The schedule for Indalloy No. 9 was designed to yield a time/temperature cycle, relative to the melting temperatures, similar to that for 62Sn-36Pb-2Ag in Fig. 7.

The principal objectives in selecting the schedule for the Indalloy No. 9 solder were to obtain a nearly identical time during which the substrate was hotter than the solder melting temperature and to duplicate the superheating of the solder on the substrate above its melting temperature.

Except for the differences appearing in Table 1, the procedure for specimen assembly given in Section D.1 should be followed when Indalloy No. 9 solder is used.

E. DESCRIPTION OF THE PULL-WIRE BENDING JIG

One problem area in the fabrication of test parts is the achievement of a uniform bend geometry without breaking the pad away from the substrate. At RCA, we had been clamping one jaw of a pair of small pliers across the wire and bending the wire up against that jaw while pulling the wire with a second pair of pliers to keep it straight. The jaw width of the first pair of pliers was ground to the desired lever-arm length minus one-half the wire

*Indium Corporation of America, Utica, NY.

15. R. H. Zeien, "Characterization of Thick Film Fritless Metallization," *Proc. Int. Microelectron. Symp. (ISHM), 1974*, p. 7.

TABLE 1. ASSEMBLY SCHEDULES FOR THICK-FILM-CONDUCTOR ADHESION SPECIMENS AND ASSOCIATED DATA FOR TWO SOLDERS

Solder	Alloy Sn62	Indalloy No. 9
Composition	62Sn-36Pb-2Ag	70Sn-18Pb-12In
Melting/liquidus temperature, °C	179	162
Flux	Kester 1544	Indalloy No. 4
Time during which substrate exceeds solder melting temperature, s	34	36
Substrate peak temperature, °C	222	202
Eurotherm Controller Settings		
Set point (chromel-alumel thermocouple in air-expander nozzle is the sensor), mV	18.5	14.75
Proportional band, %	2	2
Derivative setting	5	5
Integral setting	5	5
Maximum power limit (peak reading of thyristor package meter), A	∿7	∿7
Precision reading of peak current to Serpentine II heater, A	6.9	6.9

diameter (i.e., 0.050 - (0.031/2) = 0.034 in.). This method required considerable training of operators to obtain reproducible bend geometries. A fixture to eliminate subjectivity from the bending was designed. This unit, shown in Fig. 8, fits over the two wires and indexes the lever-arm length from the substrate edge. The substrate and the fixture form a bending brake with which the wire is bent around the fulcrum edge while producing a minimum of lifting forces on the test pad. Although lever-arm lengths produced by the jig depend on the accuracy of the test-pattern positioning and the precision of the substrate width, because of the simplicity of the jig design, the facility of its use, and the quality of bends it produces, RCA recommends the bending jig for use with the test method.

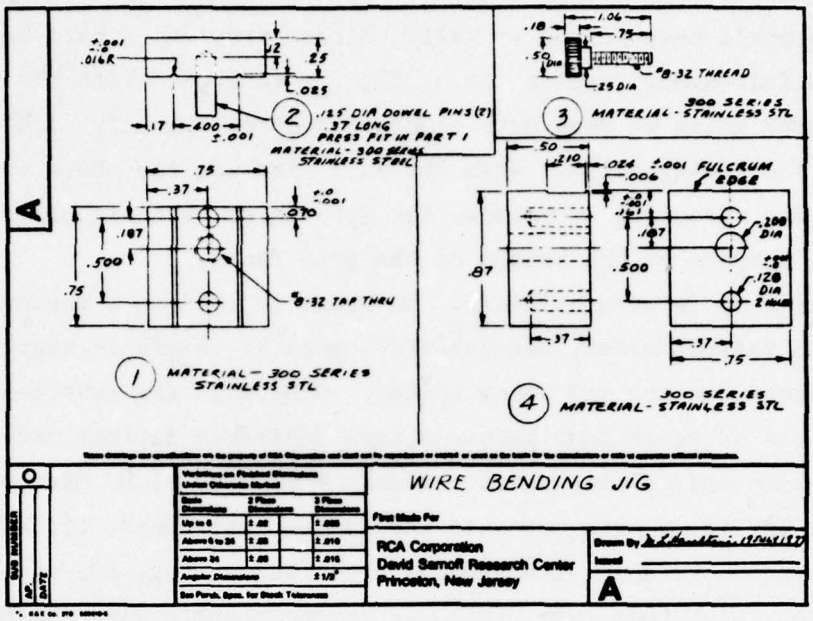

Figure 8. Pull-wire bending jig.

F. METHOD OF CUTTING THE PULL WIRES

Throughout the study, pull wires were cut with a pair of small, diagonal-cutting pliers. The pliers were ground flat across the outside surface of the jaws and to a thin edge from inside each jaw (~25° included angle). They were polished carefully so that they would introduce a minimum of compression in the wire during the cutting action. The cuts were made close to (1/16 in. from) each test pad at the substrate, with the flat face of the jaws positioned toward the test pad being prepared. The cut was made diagonally so that the plane of the cut lay at approximately 45° to the wire axis and was angled down over the test pad toward the substrate. This applied no lifting forces to the pad adjacent to the cut and minimized the shearing and lifting forces on other pads soldered along the wire.

G. SELECTION OF A TEST MACHINE AND OPTIMIZED GRIPPING

The choice of a test machine for pulling the samples was made on the basis of availability and known quality. An Instron* model TTC Universal

*Instron Corporation, Canton, MA.

Test Machine was used with an Instron 100-kg-maximum load cell. A table-model Instron would have served as well. Either provides a hard-beam test apparatus and full-scale readings of 5, 10, ... to 200 lb with the 100-kg cell. The upper grips we used were standard Instron manually tightened grips designed for the 100-kg cells. When the pull wire was too short to be held with these grips directly, we shimmed the grip faces at their top so that the wire could be gripped at the bottom of the grip faces.

The lower grip is more critical. In order to achieve a maximum number of the desired failure modes, the substrate must be carefully supported immediately adjacent to the pad being tested. Otherwise the substrate may break during the adhesion test before a more desirable failure mode can occur. A Universal clamp and leveling device from a Tukon* Model MO Microhardness tester, shown in Fig. 9, was mated to the Instron crosshead, fitted with special substrate hold-down like the one described in Fig. 10, and used as the lower grip. With this grip, failures in the ceramic were minimized and testing was straightforward.

*Wilson Instrument Div., ACCO, Bridgeport, CT.

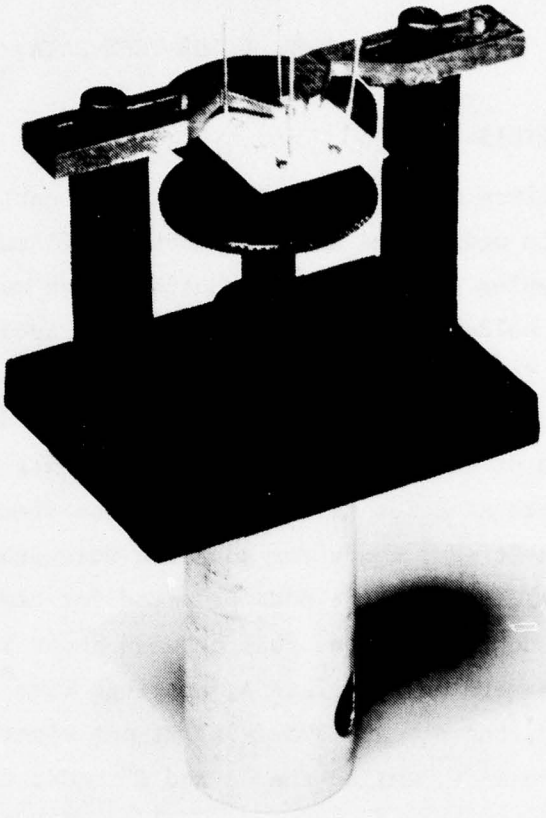

Figure 9. Lower grip, with specimen ready for test (shown approximately full size).

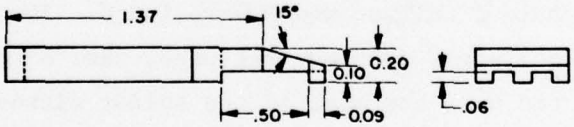

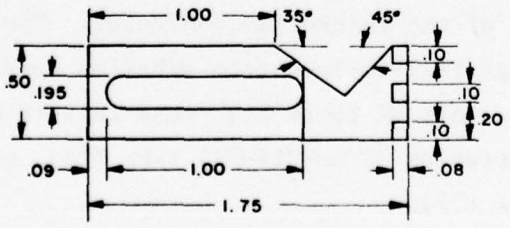

NOTE: LEFT-HAND HOLD-DOWN SHOWN
RIGHT-HAND HOLD-DOWN IS MIRROR IMAGE

Figure 10. Low-grip specimen hold-down (dimensions in inches).

SECTION III

INTERPRETATION OF THE TEST DATA

A. FAILURE MODE ANALYSIS

A variety of failure modes were observed in our earlier study of Au-Pt inks [13]. For low to medium-low adhesion-strength films, the minor stresses caused by loading samples into the test machine caused many failures; in these, invariably the film, solder, and wire broke from the substrate in one piece. With medium-strength films, the failed part had about the same appearance, but most specimens could be tested and yielded quantitative data. We have designated this appearance of failure as an "A" failure mode. It indicates a thick-film-to-substrate adhesion failure. It can be clearly seen that in earlier studies of Au-Pt(-Pd) conductor adhesion strength [13], which have been analyzed in Fig. 11(a), most of the pads prepared for testing failed with an "A" failure mode if the failure load fell between about 2 and 9 lb. This was the case if the films were on substrate A, American Lava* 614 (96 wt pct alumina), or substrate D, Coors** ADS 995 (99.5 wt pct alumina). At higher loads a second major failure mode, called the "A and C" mode, was seen. With this mode, part of the thick-film pad was removed along with the wire and some of the solder, but the film-to-substrate adhesion strength was too high for the complete removal of the film.

Two other high-load failure modes were found. In the interpretation of the soldered-wire peel-test specimen failures, the "B" mode is characterized by the removal of the wire and most of the solder without the removal of the thick-film pad, indicating that the solder-to-conductor interface was the weakest area stressed by the test procedure. A "C" mode failure results when the pull wire tears through the solder pad, leaving most of the solder behind and not removing any of the thick-film conductor. The occurrence of the "C" mode indicates a high film-to-substrate adhesion and/or too little solder or too weak a solder. All of these high-load failure modes were observed in adhesion testing studies of Au-Pt(-Pd) inks [13], as well as in an earlier study of copper inks [12].

*American Lava Div. of 3M Co., Chattanooga, TN.
**Coors Porcelain Corp., Golden, CO.

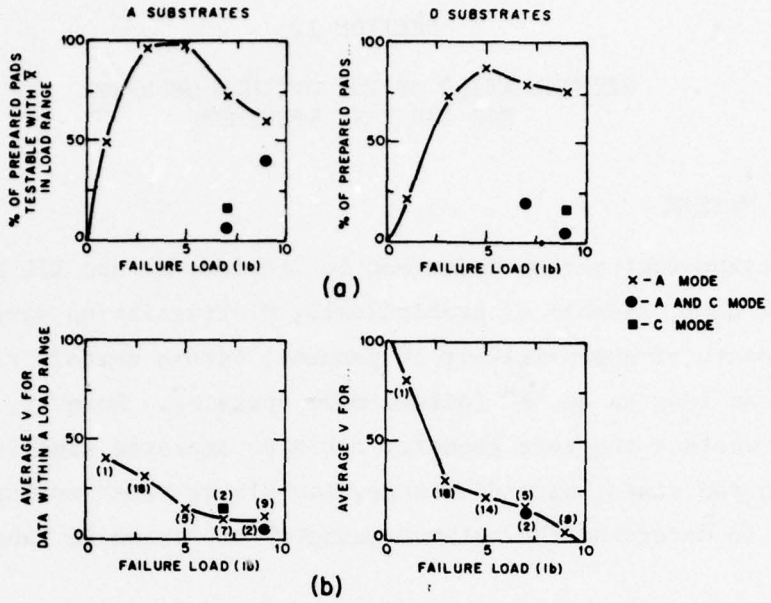

Figure 11. Analysis of adhesion test data from Au-Pt(-Pd) inks on 96 and 99.5 wt pct alumina substrates.

B. TEST DATA ANALYSIS

Figure 11(b) indicates that the average V* for A-mode failures (i.e., the expected value of V for a sample group with their $\bar{X}$'s falling within a failure load range) was not increased by the onset of failure modes other than "A", as long as the A-mode data are segregated. The number of $\bar{X}$'s (sample lots) contributing to a point is shown in parentheses adjacent to the data point. From Fig. 11(b), it is clear that for both substrates A and D the average V falls below 25 percent, once the low range (0 to 4 lb) of the failure loads is exceeded.

---

*$\bar{X}$ is the arithmetic mean of the Instron-measured failure loads of a specimen lot of size N. The coefficient of variation, V, is the standard deviation, σ, divided by $\bar{X}$ and expressed in percent. In Fig. 11, the $\bar{X}$ and σ values were calculated from the failure loads and the number of tests from which each $\bar{X}$ was obtained. More specifically, whenever any of the prepared pads of a sample lot could be tested, the test-failure-load values obtained determined the $\bar{X}$ (and the load range) for the lot. When no pads from a sample lot could be tested, the lot was assigned an $\bar{X}$ of zero. The intended sample size in the study [13] was 12 pads for A substrates and 8 pads for D substrates.

SECTION IV

DETERMINATION OF THE OPTIMUM GEOMETRY FOR THE TEST SPECIMEN

A. THE TEST MATRIX

The adhesion test method described in Sections II and III had proved a highly useful test, capable of statistically distinguishing variations in adhesion strength of approximately 10 percent, within certain ranges of failure strength and as long as an "A" failure mode operates. However, it was desirable to determine whether the test geometry could be improved significantly. The metallization pad sizes, wire diameters, and "lever arms" evaluated in this study matrix to determine the optimum geometry are shown in Table 2.

TABLE 2. ADHESION TEST PARAMETERS

Wire Parameters			Test-Pad Size ($in.^2$)	Lever-Arm Size** (in.)
Diam. (in.)	→	Hardness (KHN_{25})*		
			0.250 x 0.250	0.020
0.020	→	105	0.150 x 0.150	0.035
0.032	→	106	0.100 x 0.100	0.050
0.041	→	95	0.080 x 0.080	0.060
			0.060 x 0.060	0.080

*25-g load Knoop microhardness measurements were made on a Tukon Model MO Tester.
**Distance from loading axis to edge of pad.

Specimens were made with permutations of the Table 2 variables, using 200-mesh prints of three Au-Pt(-Pd) inks studied earlier [13]. Each of these was fired at a particular peak temperature to yield films with moderately high, medium-high, or low adhesion strengths. These three conductor film-firing combinations were used as vehicles to study the effects of test-specimen-element size variation on the failure loads and fracture modes of the test specimens.

Two variables other than those enumerated in Table 2 are the amount of solder and the amount of flux. The amount of solder was determined by calculation to be two times the amount that would be required to form a triangular prism shape around the wire, where the metallization pad is the base of the prism and the two top faces of the prism lie tangent to the wire and meet to form an edge parallel to the wire axis and with the same length as the metallization pad width. This relative amount of solder is the same as that used throughout the NASC study [13] for 0.10-in. x 0.10-in. pads with 0.032-in. diameter wire. For a few singularities in the matrix, such as the largest wire diameter on the smaller pads, the above method of determining solder volume was not used (see Table 3). The solder composition was 62Sn-36Pb-2Ag.

TABLE 3. LENGTHS OF SOLDER USED FOR VARIOUS PAD AND WIRE COMBINATIONS

Test-Pad Size ($in.^2$)	Pull-Wire Diameter (in.)		
	0.041	0.032	0.020
0.250 x 0.250	2.58	2.16	1.45
0.150 x 0.150	0.79	0.68	0.47
0.100 x 0.100	0.45*	0.26	0.190
0.080 x 0.080	0.26*	0.151	0.110
0.050 x 0.050	0.129	0.072	0.040

*Length not calculated by method described in text.

Kester 1544 flux was metered with a Finnpipette Model FP-11.* A volume of 7 µL flux was used on all 0.1-in. x 0.1-in. and smaller pads; 14 µL was used on 0.15-in. x 0.15-in pads. On 0.25-in. x 0.25-in. pads, 21 µL of flux was used.

*Variable Volumetrics, Woburn, MA.

The data from the study of test-element sizes are shown in Figs. 12 through 23. From Figs. 12, 13 and 14, it can be seen that the variation of failure load is a direct function of the test-pad width, as long as only A-mode failures are considered. (Note that all the failure data are "A" mode in Figs. 12-23 except where otherwise indicated.) The fit of the data to a straight-line form is excellent. A perfect fit corresponds to $r^2 = 1.0$, where r^2 is the coefficient of determination of the line. Values of r^2, the slope of each line, and its intercept were calculated using Hewlett-Packard's SD-03A curve-fitting program with their model HP-97* calculator.

B. TEST RESULTS AND DISCUSSION

Two important conclusions can be drawn from the good fit of the data to straight lines. First, the often used concept that the failure load, F, for the soldered-wire peel test can be expressed as a stress,

$$S = \frac{F}{A} \tag{1}$$

where A is the area of the conductor pad, is erroneous. For any film studied, the data do not fit a curve of the form $F = K_1 A$ nearly as well as they fit the form $F = K_2 W$, where K_1 and K_2 are constants and W is the width of a square pad. Thus, the test is a peel test and as such is more properly described in terms of force per unit width rather than per unit area. Accordingly, a first-order normalization of a failure load, F_1, taken with a nonstandard pad width, W_1, can be made according to

$$F_2 = \frac{W_2}{W_1} F_1 \tag{2}$$

where W_2 is the standard test-pad width.

This should be particularly effective where W_1 and W_2 are close (i.e., for 0.080-in.- and 0.10-in.-wide test pads).

*Hewlett-Packard Corp., Palo Alto, CA.

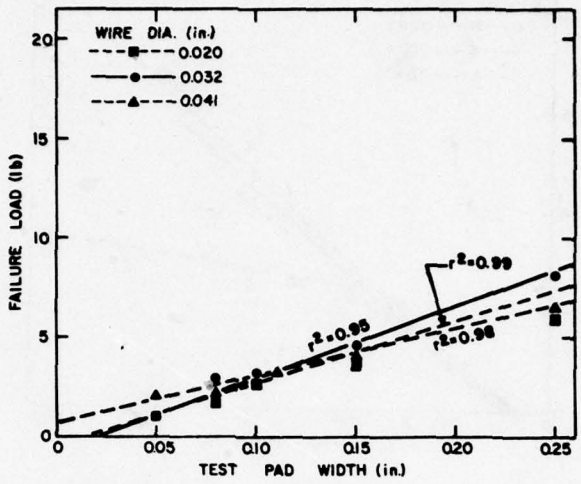

Figure 12. Variation of failure load with test-pad width and pull-wire diameter for a low-adhesion-strength film (reactively bonded Au-Pt ink No. 9, 200-mesh printed, purposely underfired at 850°C for 10 min to achieve a low, but measurable, adhesion strength).

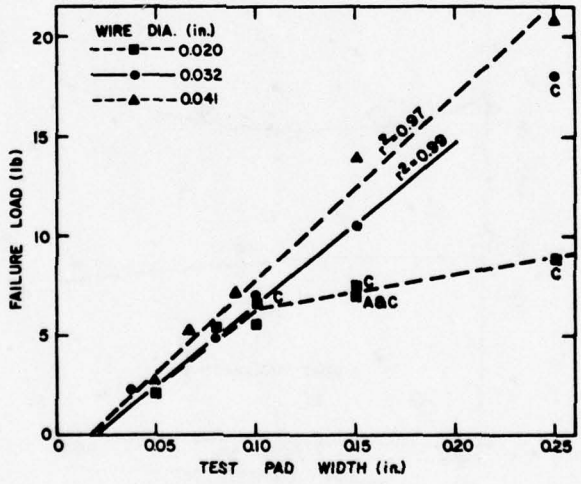

Figure 13. Variation of failure load with test-pad width and pull-wire diameter for a high-adhesion-strength film. (Frit-bonded Au-Pt-Pd ink No. 10, 200-mesh print, fired at 925°C for 10 min.)

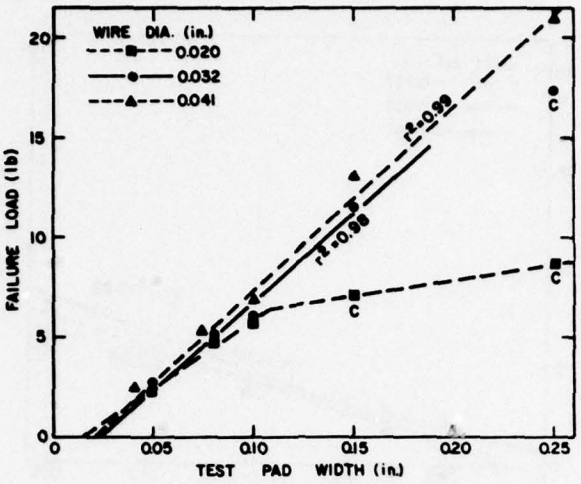

Figure 14. Variation of failure load with test-pad width and pull-wire diameter for a high-adhesion-strength film. (Frit-bonded Au-Pt-Pd ink No. 18, 200-mesh print, fired at 925°C for 10 min.)

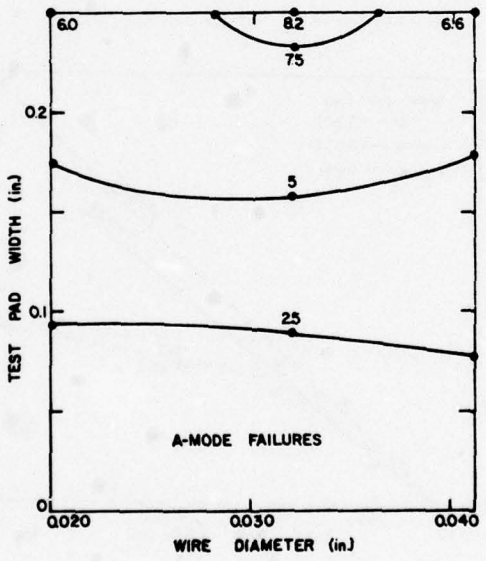

Figure 15. Isoload curves and failure-mode regimes for a matrix of test-pad widths and pull-wire diameters for weakly adherent, reactively bonded Au-Pt film No. 9.

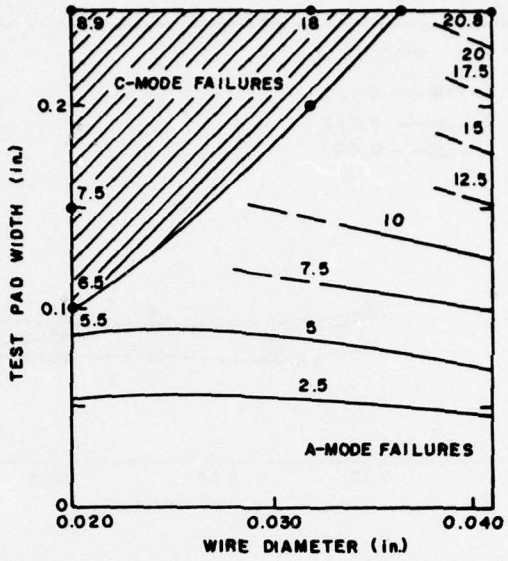

Figure 16. Isoload curves and failure-mode regimes for a matrix of test-pad widths and pull-wire diameters for strongly adherent, frit-bonded Au-Pt-Pd film No. 10.

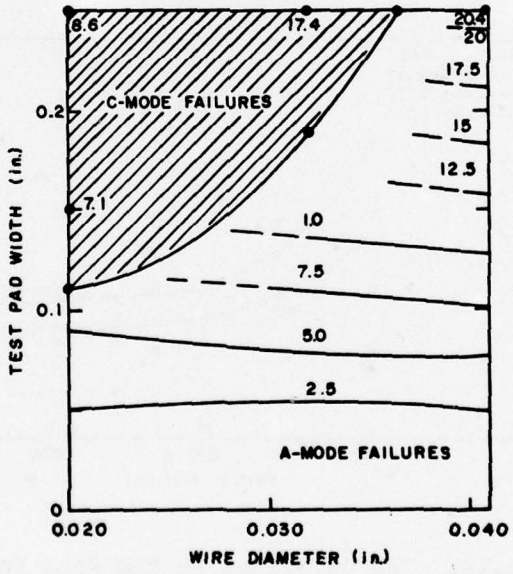

Figure 17. Isoload curves and failure-mode regimes for a matrix of test-pad widths and pull-wire diameters for strongly adherent, frit-bonded Au-Pt-Pd film No. 18.

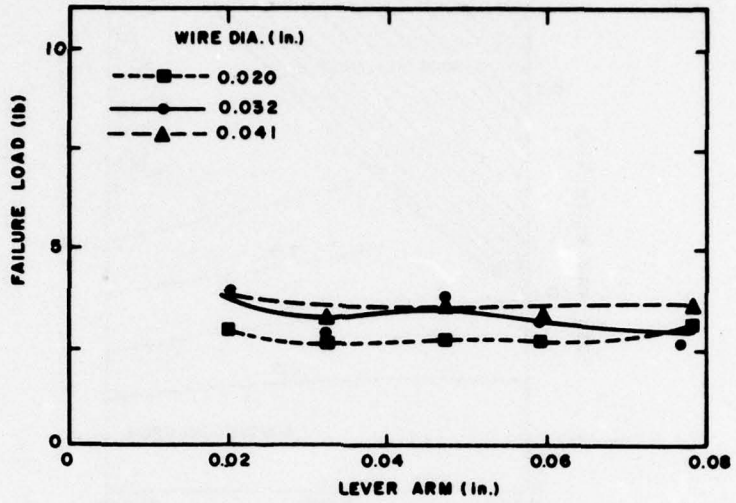

Figure 18. The effect of changing lever-arm and wire diameter on the failure load for reactively bonded Au-Pt film No. 9.

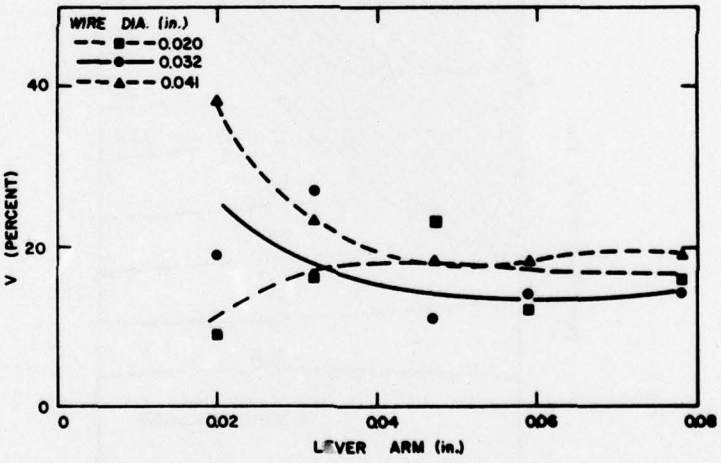

Figure 19. The variation in the data in Fig. 18 as a function of the lever-arm and wire diameter.

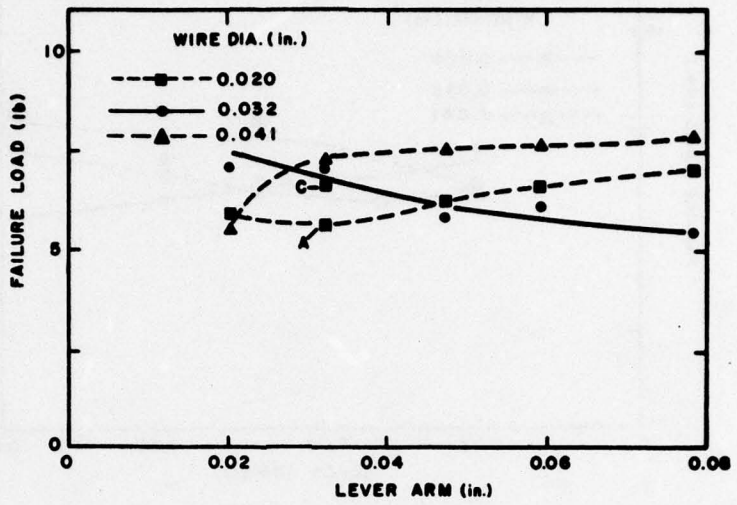

Figure 20. The effect of changing lever-arm and wire diameter on the failure load for frit-bonded Au-Pt-Pd film No. 10.

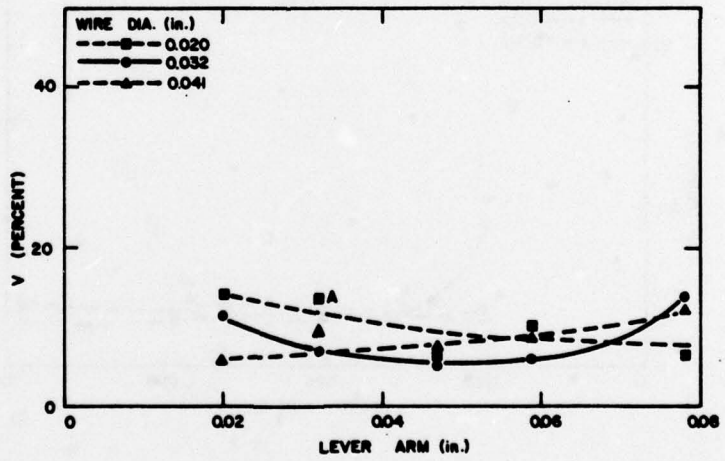

Figure 21. The variation in the data in Fig. 20 as a function of the lever-arm and wire diameter.

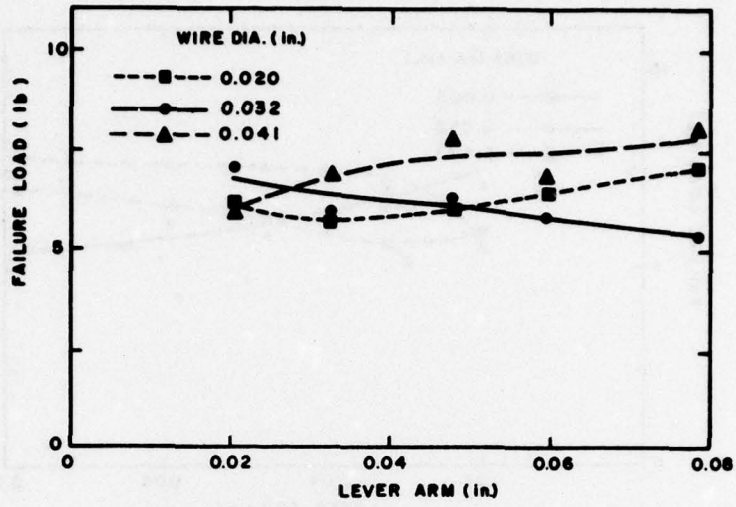

Figure 22. The effect of changing lever-arm and wire diameter on the failure load for frit-bonded Au-Pt-Pd film No. 18.

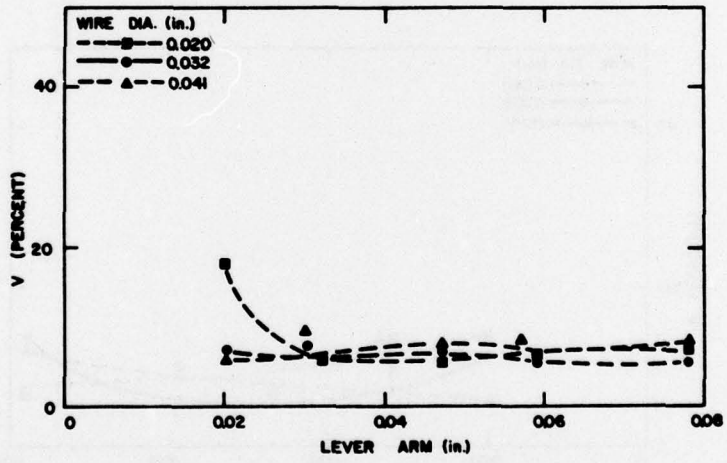

Figure 23. The variation in the data in Fig. 22 as a function of the lever-arm and wire diameter.

A more precise normalization scheme would take into account the fact that the intercept of the curve on the y axis is not zero, as implied by Eq. (2). However, further study of the test will be necessary to formulate a universal normalization formula that can compensate for both effects.

The second conclusion (discerned from Figs. 13 and 14) relates to the effect of the wire diameter. As this is reduced, the load it can hold before tearing through the solder (i.e., before the onset of C-mode failure), decreases with the wire diameter for a given test-pad size. The increase in the C-mode failure load with test-pad size is judged to be due to a greater depth of solder through which the wire must tear. For the same pad and solder "bump" size, C-mode failure loads are expected to remain approximately constant, no matter how much the film-to-substrate adhesion strength increases above the level at which C-mode failures begin.

A wire diameter of 0.041 in. will give higher failure loads than an 0.032-in. wire diameter before the onset of C-mode failure. However, although Au-Pt inks 10 and 18, as-fired, are high-adhesion-strength materials, their adhesion strengths still lie well within the A-mode failure regime of an 0.10-in. x 0.10-in. pad soldered to an 0.032-in.-diameter pull wire. Figures 15 through 17 make this more apparent. These figures illustrate isoload curves within the A-mode failure regime of a matrix of specimen lots of various pull-wire diameters and pad widths. The boundaries between the A and C regions and the positions of the isoload failure-strength curves were calculated by linear interpolation between adhesion-failure load values and by studying the number of specimens failing by each failure mode for adjacent matrix points. The values on the isoload curves and other failure loads are given in pounds. Matrix-point failure loads are given in the C region, because insufficient C-mode failures were observed to calculate isoload curves. Lever-arm lengths were 0.050 in. for the data shown in Figs. 15-17.

Figures 18-23 present the data from the study of the variation of the lever-arm length and pull-wire diameter for a constant test-pad width of 0.10 in. Only marginal effects can be observed in the failure-load data. Comparison of the failure loads with the data variation for the same ink (e.g., Fig. 18 with Fig. 19) shows a striking correlation. In Fig. 18 no clear trends can be detected, although one might suggest that the smallest wire diameter gave lower failure loads and the smallest lever arms gave higher loads. There

is a much clearer effect in Fig. 19, viz., larger wire diameters and small lever arms cause a high variation. Note that the lowest V's tend to be approximately 18 percent for this purposely underfired, weakly adherent film. For the more strongly adherent films of inks 10 and 18, the failure-load data of Figs. 20 and 22 show the trends indicated in Fig. 18 (i.e., the 0.020-in.-diameter wire produces the lowest failure loads, at least for lever arms below approximately 0.050 in.). Figures 21 and 23 show the variation in the data of Figs. 20 and 22, which clearly indicates the reduction in V for an increase in failure load (discussed in Section III.B). Obtaining a low V in a data group requires the separation of the various failure modes before statistical analysis. In adhesion failure data, V's of 10 percent or less are judged to be excellent.

C. CONCLUSIONS

The results of the work may be summarized as follows:

The "standard" solder-wire, tensile peel test, in which an 0.1-in. x 0.1-in. conductor pad, an 0.032-in.-diameter soft copper wire, and an 0.050-in. lever arm are used, is a good choice of sample geometry. It gives highly reproducible failure loads and well-behaved modes of failure over a wide range of film-adhesion strength. The geometry of the du Pont dip-soldered variation of the test, with the conductor pad size of 0.080 in. x 0.080-in. being the major difference from our test geometry, is also good. The 0.080-in. x 0.080-in. pad size is preferable to the 0.10-in. x 0.10-in. size for the du Pont method of soldering (i.e., dipping the substrate with the pull wires attached) with respect to retaining a sufficient amount of solder on the pad. Much larger or smaller conductor test-pad sizes or wire diameters are unacceptable because they either made sample assembly difficult or increased the incidence of failure modes other than the most desirable (adhesive) failure mode (i.e., the "A" mode, where thick-film pad, solder, and wire are torn together from the substrate by the test loading).

The effect of varying the lever-arm length was not as straight-forward. Earlier work had indicated that, in some cases, longer lever arms gave lower failure loads. The effect was not verified by this part of the study. Perhaps this was because the films studied did not include one of medium adhesion

strength. It appears clear, on the other hand, that where the adhesion strength of a film is so great that the wire is reshaped during the test procedure, the effect of the lever arm should be negligible, and this model is supported by the data.

The standard variations of the failure loads divided by the mean load for each group were generally well behaved ($\tilde{\sim}$10% or less) except for the low-adhesion-strength conductor films. Thus, it is unlikely that any significant lever-arm effect present in our data could have escaped detection.

SECTION V

CORRELATION OF DATA FROM DIFFERENT TEST METHODS

In addition to obtaining the normalizations of data from soldered-wire peel tests with different pad sizes, described in Section IV, it was desirable to study the practicability of correlating the data from the soldered-wire peel test with another adhesion test method.

The thermocompression (TC) peel test, used to test gold and silver conductor adhesion strengths [1,11,12], was of interest. Soldered-wire peel test parts from the original sample lots studied in a 1974 Naval Air Systems Command Contract [11] were prepared; Indalloy No. 9 solder was used on the gold conductor and both 62Sn-36Pb-2Ag and Indalloy No. 9 were used on the silver conductors. The data obtained are shown in Figs. 24 and 25. For some data points, it may be noted in these figures that leader lines are shown between the symbols and the points where the symbol would have been plotted, had space permitted.

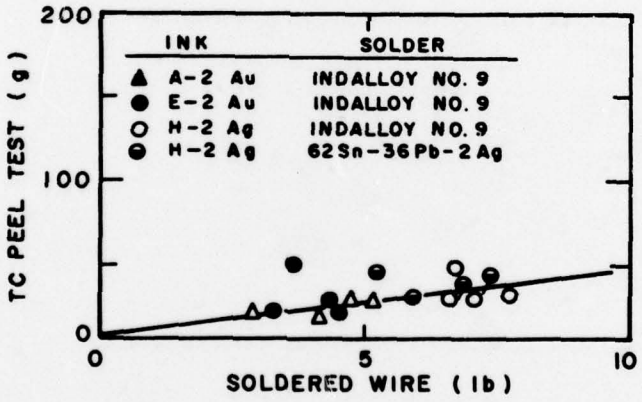

Figure 24. Correlation between adhesion-strength values measured by TC-peel and soldered-wire tests - frit-bonded inks.

It is obvious from the figures that a simple direct proportionality between the data values of the two tests is erroneous. Separation of the frit-bonded data from the mixed-bonded and reactively bonded data yielded nominally sensible data variations, which appear to be useful for first-order

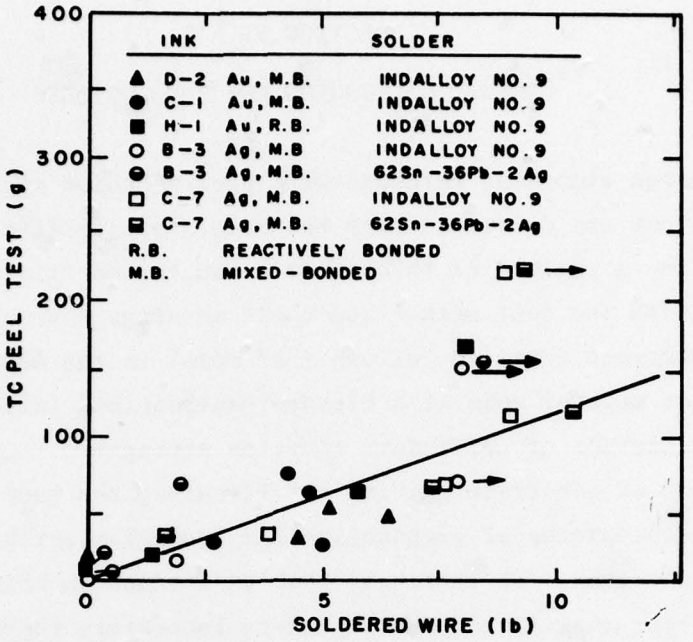

Figure 25. Correlation between adhesion-strength values measured by TC-peel and soldered-wire tests - reactively bonded and mixed-bonded inks. (A data point with an arrow indicates a failure type other than A-mode.)

correlations. The requirement for separating the frit-bonded data from the rest is believed to be due to the high shear stresses at the failure interface during the TC bonding. Frit-bonded films are believed to be more sensitive to these stresses. There appears to be little separation between the gold and the silver ink data within either of the two figures.

First-order correlation of data between the two tests can be made on the basis of Figs. 24 and 25 if (1) the failure modes are handled correctly, (2) the bonding type is known, and (3) caution is observed.

SECTION VI

GENERAL DISCUSSION AND CONCLUSIONS

The suggested standard, soldered-wire peel-adhesion test method developed under the contract and described here has been shown to give well-behaved peel-strength data for a variety of thick-film conductor materials. Failure modes that are seen with the test method and their meanings have been discussed. The film-to-substrate adhesion failure ("A" mode) is the most meaningful, but the occurance of another mode at a higher-than-required failure load can be taken as an indication of sufficient adhesion strength.

The methods of substrate heating and fixturing the test specimen for assembly and the techniques of preparation for testing described in this report are strongly advocated. It is likely that variations on this test method can be devised without sacrificing laboratory-to-laboratory reproducibility of the data, as long as the substrate thermal history, specimen geometry, and materials parameters remain constant. It should make little difference whether the heat is applied by hot air or a belt oven, for instance. However, matching the substrate time/temperature cycle from another heat source to that from the hot-air soldering technique may prove troublesome.

If a high rate of test-specimen production is required, a system of indexing previously jigged parts over a hot-air nozzle can be easily designed, but it is important that the specimens not be moved while the solder is near its solidification temperature.

It is again emphasized that the sequential testing of pads along a pull wire is poor practice, unless the pads to be tested subsequently have been isolated from the pad being tested by cutting the wire between them.

In the process of making a test more reproducible, it is a natural consequence that the precision of the test data will be improved. This means that a change in adhesion strength, resulting from material or processing variations, can be detected more easily (i.e., distinguished in spite of the data scatter). When the V's of two groups of data are reduced, smaller sample lots will permit the statistical justification of a decision at the same confidence level as formerly. Justification for abandoning a nominally satisfactory adhesion-measurement technique presently in use to adopt the one presented here may be found in the reduced number of manhours required to prepare and test smaller sample-lot sizes.

REFERENCES

1. T. T. Hitch, "Adhesion Measurements on Thick-Film Conductors," in K. L. Mittal, Ed., *Adhesion Measurements of Thin Films, Thick Films and Bulk Coatings*, to be published by ASTM, Philadelphia, PA.

2. L. Jacobson, "Testing for Adhesion of Hybrid Films," *Proc. IEEE and EIA Electronic Components Conf., 1971*, p. 474.

3. R. P. Anjard, "Thick Film Conductor Adhesion Testing," *Microelectron. Reliability* 10, 269 (1971).

4. S. S. Leven, "Qualification Requirements for Thick-Film Networks," ECOM Final Report No. ECOM-73-0326-F, by Westinghouse D&E Systems Center, Baltimore, MD, Oct. 1975.

5. D. R. Johnson and R. E. Knutson, "Parallel Gap Welding to Thick-Film Metallization," *IEEE Trans. Parts, Hybrids, and Packaging* PHP-12, 187 (1976).

6. A. C. Buckthorpe, "Degradation of Thick Film Conductor Adhesion," *IERE Conf. Hybrid Microelectron., 1973*, p. 57.

7. T. H. Lemon, "High Tensile Strength Thick-Film Silver-Palladium Metallizations," *IERE Conf. Hybrid Microelectron., 1975*, p. 23.

8. P. F. Becher et al., "Fracture Mechanics Approach to Thick Film Adhesion Testing," *Proc. Int. Microelectron. Symp. (ISHM), 1975*, p. 235.

9. P. F. Becher and J. S. Murday, "Factors Affecting Thick Film Adhesion," *Proc. Int. Microelectron. Symp. (ISHM), 1976*, p. 235.

10. E. I. du Pont De Nemours & Co., Inc., "Method of Test for Wire Peel Adhesion of Soldered Thick Film Conductors to Ceramic Substrates," *The Thick Film Handbook*, Section A-74672, Wilmington, DE, March 1971.

11. T. T. Hitch and K. R. Bube, "Basic Adhesion Mechanisms in Thick and Thin Films," Final Report, NASC Contract No. N00019-C-74-0270, 31 Jan. 1975.

12. T. T. Hitch and K. R. Bube, "Basic Adhesion Mechanisms in Thick and Thin Films," Final Report, NASC Contract No. N00019-75-C-0145, 30 Jan. 1976.

13. K. R. Bube and T. T. Hitch, "Basic Adhesion Mechanisms in Thick and Thin Films," Final Report, NASC Contract No. N00019-76-C-0256, 31 Jan. 1977.

14. E. J. Conlon, R. DeStephanis, and T. T. Hitch, U.S. Pat. 3,972,463 (1976) (RCA Corp.).

15. R. H. Zeien, "Characterization of Thick Film Fritless Metallization," *Proc. Int. Microelectron. Symp. (ISHM), 1974*, p. 7.

APPENDIX

DETAILS OF EXPERIMENTAL EQUIPMENT

Some effort was devoted to selecting high-quality components that are readily available at moderate cost for the test methods described in this report. An item of particular importance was the selection of a temperature-control system for the Serpentine II air heater. This controller also had to be capable of controlling the solder-pot temperature for solder dip preparation of the substrates before assembly. The unit used for the early work [12,13] was a West Gardsman* Model JP-S22 microammeter-type controller, with a 240-V, 50-A SCR output and adjustable controls for maximum voltage output and voltage control span. This power controller was designed and built by RCA several years ago. Today, several modern design, bridge-balance-thermocouple-circuit temperature controllers are available for less than $500.** Two such units owned by RCA were tested.

A Thermoelectric† Model 400 Controller was found to be unsatisfactory, despite its capabilities for proportional band reset operation. It does not have the derivative feature of "rate" (i.e., the ability to sense how fast the temperature is approaching the set point and automatically adjust the power output to minimize undershoot or overshoot). That lack is considered the most important reason for its limited performance. On that basis, the choice of controllers was limited to those that have proportional band, adjustable automatic reset, and adjustable rate features. A Eurotherm†† Model 090 (Model 900 is the presently available equivalent) with the above features and adjustable maximum power was tested and found satisfactory. However, the precision of control possible with this controller, $\pm$0.001 mV, is much finer than is required for the purpose of building soldered, adhesion-test samples.

*West Gardsman Div. of Gulton Industries, Inc., Chicago, IL.

**These prices include the solid-state switching devices, such as SCRs, triacs and their drive circuitry, which are necessary for the control of power to heating elements.

†Thermo-Electric Co., Inc., Saddle Brook, NJ.

††Eurotherm Ltd., Worthington, Sussex, G.B.

For a chromel-alumel thermocouple sensor, 0.001 mV corresponds to ~0.025°C. Lower-precision, and correspondingly lower-priced, controllers manufactured by Eurotherm* in the United States are available. Their Model 919, priced near $500, was procured and tested, and proved to be satisfactory. Closely equivalent Models No. 917 and No. 918 also would be satisfactory. Another controller, the Theall** Model TC-1000, is available with proportional band, adjustable rate, adjustable maximum power, and adjustable automatic reset. It also appears capable of satisfactory performance, at a modest price, but was not tested.

Electrical control circuitry to simplify the reproduction of heating cycles was developed by a series of iterations. The simplest of these is described by the schematic in Fig. A-1. If an apparatus must be operated from 208 V ac, as ours was, a transformer is required to boost the peak output voltage to about 240 V ac. It should be wired between the Serpentine heater and the power leads shown leading to it from the relay and the thyristor unit in Fig. A-1.

A list of acceptable parts for the circuitry described in Fig. A-1 is included in Table A-1.

*Eurotherm Corp., Reston, VA.
**Theall Engineering Corp., Oxford, PA.

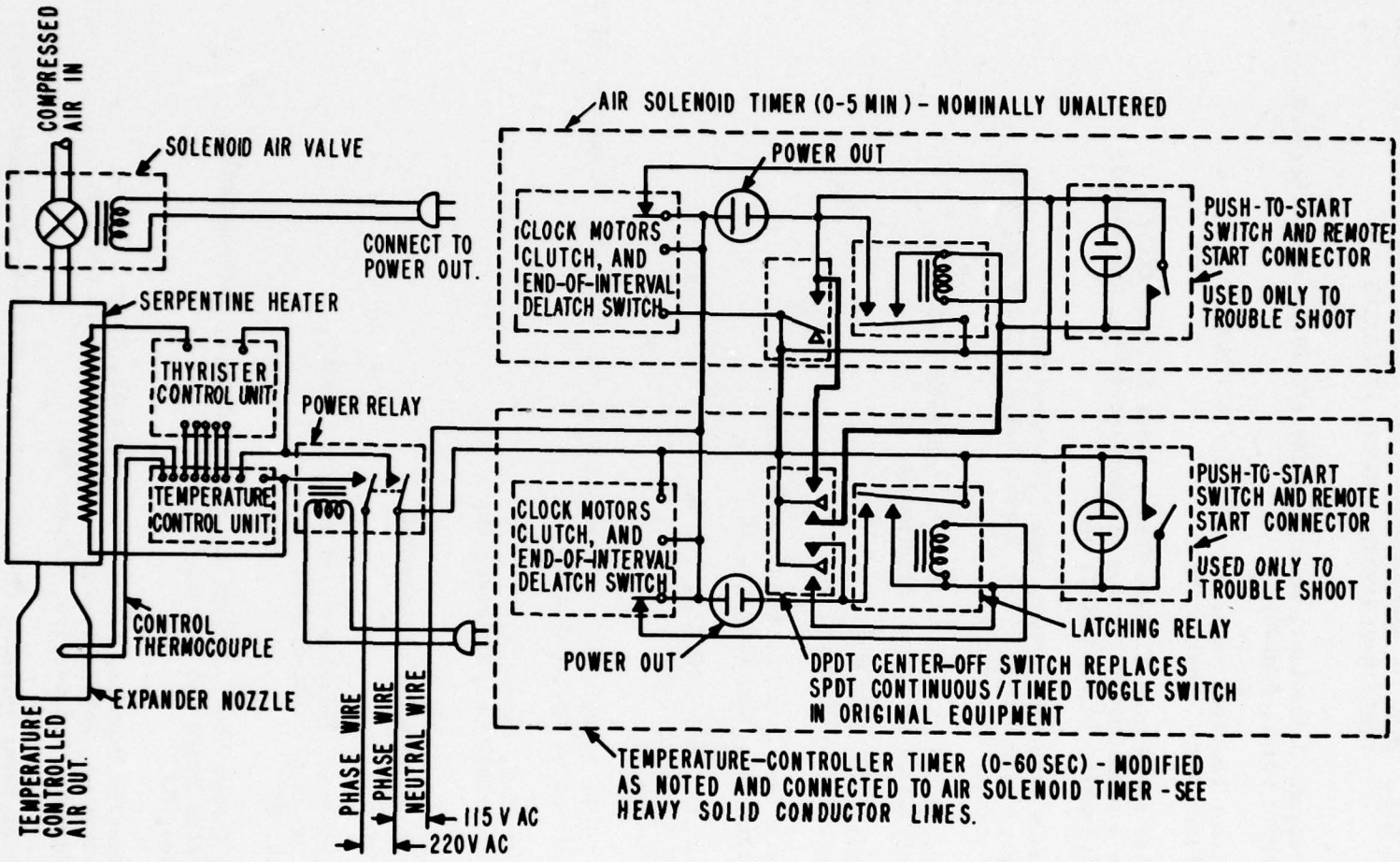

Figure A-1. Soldering-cycle time/temperature control apparatus (schematic diagram).

TABLE A-1. LIST OF RECOMMENDED PARTS AND MATERIALS FOR SOLDERING-CYCLE TIME/TEMPERATURE CONTROL APPARATUS

1. Temperature Controller, Model 919/PAP/K/0-29.99 mV/P10/HL/VT/X,
   Eurotherm Corp., Reston, VA

2. Thyristor Package, Model No. 031/25A/240V/M/BB/X,
   Eurotherm Corp., Reston, VA

3. Gas/Air Serpentine II Heat Torch, Model No. CGH 117575,
   Style A with 2000 W heating element, Model No. CHE 124765,
   GTE Sylvania, Inc., Exeter, NH

4. Variable Autotransformer, Type 1226 Powerstat,
   Primary volts 230/115 V ac, output volts 0-270 V ac, 9 A,
   The Superior Electric Co., Bristol, CT

5. Timers, Models No. P-1M (1-60 s) and P-5M (0-5 min),
   Industrial Timer Corp., Parsippany, NJ

6. Air Solenoid Valve, Type 21,
   Versa Valve, Englewood, NJ

7. Power Relay, Cat. No. 2600U-DPDT-120A,
   Guardian Electric, Chicago, IL

8. Solder Pot, Model MP 4AX, 800 W,
   WAAGE Electric Inc.
   Kenilworth, NJ

9. Solid-Wire Solder, 62Sn-36Pb-2Ag pct by wt, 0.031-in.-diameter: Alloy Sn62,
   Kester Solder Co., Chicago, IL

10. Solder Flux, Kester 1544,
    Kester Solder Co., Chicago, IL

11. Solder, Indalloy #9,
    Indium Corporation of America,
    Utica, NY

12. Solder Flux, Indalloy No. 4 Electro (rosin),
    Indium Corporation of America,
    Utica, NY

13. OFHC Copper Wire, 20-Gage (0.032-in. diam.), soft-annealed,
    Atlantic Brass and Copper,
    Linden, NJ

14. Volumetric Pipette, Finnpipette, Code 11, Range 5-50 µL,
    Lab Systems, Helsinki, Finland (distributed in the U.S.
    by Variable Volumetrics, Woburn, MA

15. Heat Diffuser Screens, 40-mesh nichrome, 0.010-in.-diameter wire,
    Newark Wire Cloth Co.,
    Newark, NJ